

UCRL- 84149
PREPRINT

CONF-8006169-1

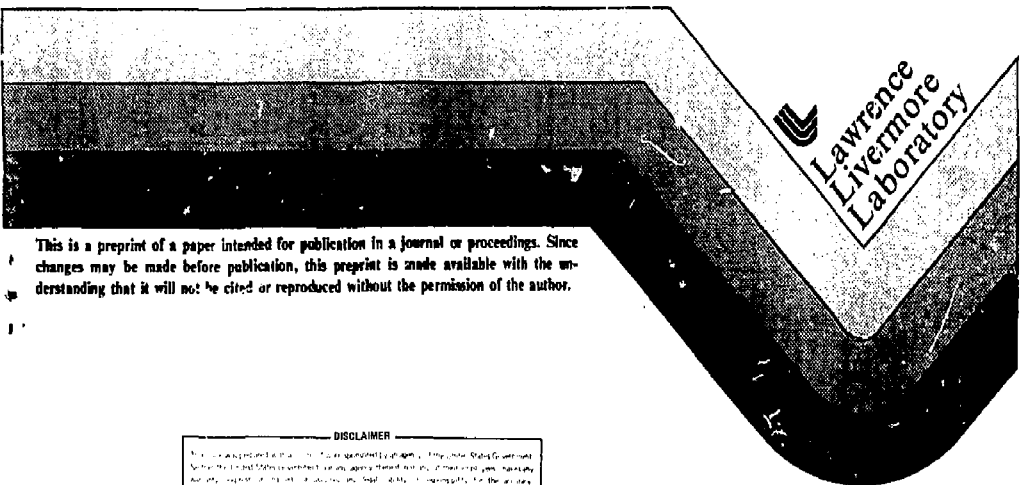
MASTER

Analysis of Multipass Laser Amplifier
Systems for Storage Laser Media

James F. Harvey

For presentation at the 1980 Army
Science Conference at West Point, New York
17-19 June 1980

25 March 1980



This is a preprint of a paper intended for publication in a journal or proceedings. Since changes may be made before publication, this preprint is made available with the understanding that it will not be cited or reproduced without the permission of the author.

DISCLAIMER

This document is prepared for the U.S. Government by Lawrence Livermore National Laboratory under contract number W-7400-ENG-48 with the U.S. Department of Energy. The U.S. Government is authorized to reproduce and distribute reprints for government purposes not withstanding any copyright notation that may appear hereon.

DISTRIBUTION OF THIS DOCUMENT IS UNLIMITED

Analysis of Multipass Laser Amplifier
Systems for Storage Laser Media

James F. Harvey

For presentation at the 1980 Army
Science Conference at West Point, New York
17-19 June 1980

* Work performed under the auspices of the U. S. Department of Energy by
the Lawrence Livermore National Laboratory under contract number
W-7405-ENG-48.

31659

Abstract

The performance characteristics of single pass and multipass storage laser amplifiers are presented and compared. The effects of the multipass amplifier parameters on the extraction characteristics are examined. For a wide range of conditions the multipass amplifier is found to provide high energy gain and high efficiency simultaneously. This is a significant advantage over the single pass laser amplifier. Finally, three specific storage laser amplifier systems, flashlamp pumped V:MgF₂, XeF laser pumped Tm:Glass, and photolytically pumped Selenium^{en}, are examined. The performance characteristics for each of the three systems are calculated and compared.

I. Introduction

Highly efficient short pulse high power lasers have many potential applications, including laser fusion drivers. One technique for achieving high powers in short pulses is to use a storage laser amplifier. A storage laser amplifier uses a laser medium with a long lived upper laser level. The upper laser level can accumulate energy from a pumping source over a relatively long time. This stored energy is then extracted by stimulated emission over a relatively short time. Examples of such storage laser media are Nd:YAG, Nd:Glass, V:MgF₂, Tm:Glass, CO₂, and Group VI media (e.g. Sulfur^u and Selenium).

The single pass amplifier system depicted in figure 1 (top) is the simplest approach to amplifying a laser light pulse. The laser beam is passed once through the laser medium. The beam is amplified as it extracts energy stored in the medium's upper laser level. The

single pass amplifier performance is limited in that it cannot simultaneously provide high energy gain and high efficiency. Under certain conditions these limitations can be overcome by using a multipass system such as the one depicted in the lower part of figure 1.

In this paper a single pass amplifier will be investigated first using the Frantz-Nodvik theory of short pulse laser amplification.^{1,2} The multipass system will then be treated by sequentially applying the single pass extraction equations for each extraction pass. In order to find the gain for each extraction, the changes occurring in the laser medium and in the laser beam fluence between extraction passes are determined using a simple three level laser kinetics model. The single pass and multipass results are compared to determine when a multipass system has an advantage over the single pass amplifier. The effects of the variation of different medium and system parameters on amplifier performance are then discussed. Finally several specific storage amplifier systems which are candidates for laser fusion drivers are discussed.

II. Single Pass Extraction

In this section the extraction characteristics of a single pass amplifier are considered. The analysis to calculate the single pass extraction performance characteristics is developed. For practical systems the pulse length and extraction period are generally short compared with the upper and lower level lifetimes, τ_2 and τ_{1x} respectively. This condition on the lower level lifetime is called "bottlenecked" extraction. For this period then the only changes in the upper and lower laser level populations, n_2 and n_1 , are due to the stimulated transitions induced by the photon field of the laser beam. The rate equations for the populations of the two laser levels and the photon field become:

$$(1/c) \partial I / \partial t + \partial I / \partial z = dI / dz = \alpha I \quad (A1)$$

(And)

$$\partial n_1 / \partial t = -\alpha I / \tau_{1x}, \quad (A2)$$

where the laser beam propagation is in the z direction and I is the intensity of the laser light. The gain coefficient, α , is defined by:

$$\alpha \equiv \sigma [n_2 - (g_2/g_1) n_1], \quad (A3)$$

where σ is the cross section for stimulated emission and g_2/g_1 is the upper to lower level degeneracy ratio. The amplifier medium loss is generally negligible. The saturation fluence, χ is defined as:

$$\Gamma_s \equiv h\nu / [\sigma (1 + g_2/g_1)], \quad (A4)$$

where $h\nu$ is the energy of the laser photon. Eqns. (A1) and (A2) can be solved to give:

$$\Gamma^0/\Gamma_s = L_n \left[\exp \left(\int_0^L \alpha_0(t_e) dz \right) \left\{ \exp(\Gamma^i/\Gamma_s) - 1 \right\} + 1 \right] \quad (A5)$$

In this equation Γ^i is the laser pulse energy fluence and is defined as:

$$\Gamma \equiv \int_{-\infty}^{\infty} I(z, t) dt. \quad (A6)$$

Γ^i and Γ^0 are the input and output fluences respectively. The small signal gain coefficient, α_0 , in the gain-length integral is the gain immediately prior to extraction and is evaluated at the time t_e of extraction.^{1,2}

The output fluence thus depends only on the input fluence normalized by the saturation fluence and on the integral of the gain along the amplifier axis. It does not depend on the specific distribution of the gain along the amplifier axis.

Equation (A5) for the output fluence has two limiting forms:

$$\Gamma^o/\Gamma_s \rightarrow (\Gamma^i/\Gamma_s) \exp\left(\int_0^L \alpha_o dz\right) \quad \Gamma^i \ll \Gamma_s \quad (A7)$$

and

$$\Gamma^o/\Gamma_s \rightarrow \Gamma^i/\Gamma_s + \int_0^L \alpha_o dz \quad \Gamma^i \gg \Gamma_s \quad (A8)$$

For small input fluences relative to the saturation fluence, the output fluence depends exponentially on the gain-length integral. At large relative input fluences the output fluence depends linearly on the gain-length integral. This behavior can be seen in figure 2, which is a graph of equation (A5) for several possible values of the gain length integral.

The laser beam energy extraction efficiency is defined as:

$$\epsilon_{ext} \equiv (\Gamma^o - \Gamma^i) / (E_p L), \quad (A9)$$

where L is the amplifier length and E_p is the pump energy density deposited in the upper laser level. Eqn. (A9) can be rewritten as:

$$\epsilon_{ext} = (\Gamma^o/\Gamma_s - \Gamma^i/\Gamma_s) / [(1 + g_2/g_1)(\alpha_o L)_M], \quad (A10)$$

where $(\alpha_o L)_M$ is the maximum possible gain-length integral for a given pump energy density, namely,

$$(\alpha_o L)_M = (\sigma/h\nu) E_p L = E_p L / [\Gamma_s (1 + g_2/g_1)]. \quad (A11)$$

Eqn. (A10) for the extraction efficiency has the following limiting forms:

$$\epsilon_{ext} \rightarrow (\Gamma^i/\Gamma_s) \left[\exp\left(\int_0^L \alpha_0 dz\right) - 1 \right] / \left[(\alpha_0 L)_M (1 + g_2/g_1) \right] \quad (A12) \quad \Gamma^i \ll \Gamma_s$$

and

$$\epsilon_{ext} \rightarrow \int_0^L \alpha_0 dz / \left[(\alpha_0 L)_M (1 + g_2/g_1) \right] \quad \Gamma^i \gg \Gamma_s. \quad (A13)$$

Efficient extraction only occurs at input fluences comparable to or greater than the saturation fluence. For all values of input fluence a larger value of the gain-length integral will result in a larger efficiency for a given Γ^i/Γ_s . This effect of the gain-length on efficiency becomes less pronounced at higher input fluences. The factor $\int_0^L \alpha_0 dz / (\alpha_0 L)_M$ is the limiting efficiency, eqn. (A13), represents the loss due to the depletion in the gain prior to extraction. This depletion is caused by decay from the upper level population during the finite time period in which the pump energy is deposited in the upper laser level. This effect will be investigated during the discussion of the multipass system. To focus attention on the extraction period itself for now $\int_0^L \alpha_0 dz$ will be considered equal to $(\alpha_0 L)_M$. Then there is no decay from the upper level and no population in the lower level. The extraction efficiency for such a single pass is plotted in figure 3 as a function of input fluence. At large input fluence the

efficiency is limited to the value $1/(1 + g_2/g_1)$ because the net gain ~~equals~~ ^{becomes} zero when $n_2/g_2 = n_1/g_1$. The efficiency is thus very sensitive to the degeneracy ratio as shown in eqn. (A13). If the extraction period is long compared with the lower level lifetime, τ_1 , the extraction is said to be "unbottlenecked". In this case the above analysis is still valid, but a zero degeneracy ratio should be used for extraction since the lower level population will not live long enough to influence the extraction. The extraction efficiency then will not be so sensitive to the real degeneracy ratio.

Figure 3 shows that the extraction efficiency for a single pass amplifier falls rapidly from unity with decreasing P^i/P_s^i ($P^i/P_s^i < 1$). The reason for this reduced efficiency is demonstrated in figure 4, which shows the general behavior of the energy extracted per unit volume, E_{ext} , along the length of a laser amplifier for a small input laser light pulse. Initially the light pulse is in the small signal regime and experiences exponential growth. Since the amplified pulse is still small compared with the saturation fluence, it has not extracted a significant portion of the energy stored in the upper laser level. As the pulse is amplified it becomes large enough that it is extracting most of the stored upper level population. The curve of extracted energy density now approaches the available stored energy density. The energy remaining in the form of an upper laser level population after the passage of the extracting laser pulse represents unextracted energy and therefore produces a decrease in extraction efficiency. In fig. 4 the area between the horizontal line $E_{ext}/E_p = 1$ and the extracted energy curve represents the energy

left in the amplifier after the extraction process. This area is shaded for the $\Gamma_i/\Gamma_s = 0.1$ curve. In the small signal regime the pulse amplification is high, but the extraction efficiency is low. In the saturated regime the pulse amplification is low, but the extraction efficiency high. So the single pass amplifier can provide high energy gain at low extraction efficiency in the exponential growth regime. Alternatively it can provide high extraction efficiency with low energy gain in the saturated extraction regime. But it cannot obtain both high energy gain and high extraction efficiency simultaneously. Efficient extraction begins to occur for input fluence values comparable to a saturation fluence.

III. Multipass Extraction

These limitations of the single pass amplifier can be overcome by using multipass extraction as illustrated in fig. 1. In such an approach a small input fluence is amplified in the exponential gain regime, and the resulting output pulse returned into the same medium. The returned pulse has sufficient fluence to extract that part of the stored energy remaining after the first extraction pass. High energy gain can then be realized with a higher extraction efficiency than is possible from a single pass amplifier.

In order to analyze the multipass amplifier system it is only necessary to repeat the extraction calculation for Γ^0/Γ_s for each extraction pass using the appropriate values for Γ^i/Γ_s and the gain-length integral. The appropriate input fluence value for the n th extraction pass is the output fluence of the previous extraction pass reduced by the optical losses during the turnaround time, namely,

$$\Gamma_n^i / \Gamma_s = (1-T) \Gamma_{(n-1)}^o / \Gamma_s \quad n \neq 1 \quad (\text{A14})$$

where T is the optical transmission coefficient. The subscript n on a quantity indicates its value prior to or during the n^{th} extraction pass. The value of the gain-length integral to be used in the n th extraction calculation will depend on the prior changes that have taken place in the two laser level populations, n_2 and n_1 , and is given by:

$$\int_0^L \alpha_{ex}(z) dz = \sigma \left[\int_0^L n_{2n}(z) dz - (g_2/g_1) \int_0^L n_{1n}(z) dz \right] \quad (\text{A15})$$

These changes have occurred during the pumped period, during previous extraction passes, and during the optical turnaround time between previous extraction passes. The changes in the populations during an extraction pass are proportional to the energy extracted:

$$\Delta \int_0^L n_{1n} dz = -\Delta \int_0^L n_{2n} dz = (\Gamma_n^o - \Gamma_n^i) / h\nu_g \quad (\text{A16})$$

Figure 5 illustrates the model used in analyzing the laser medium. The cross section for stimulated emission between the upper

and lower excited states is σ . The population in the upper state, n_2 , is also depleted by nonstimulated transitions which may be collisional or radiative. The total rate of depletion of the upper laser level, n_2/τ_2 , is characterized by a lifetime, τ_2 . A fraction, f_{21} of this upper state decay adds to the lower laser level population, n_1 , and the remainder decays to unrelated states. The lower state is also characterized by a lifetime τ_1 , and the total rate of depletion of the lower laser level is n_1/τ_1 .

During the pumping time, τ_p , the upper laser level is populated by some form of energy deposition, e.g. flashlamp or laser light pumping in the case of most solid state lasers, photolytic bleaching-wave pumping in the case of the group VI lasers, and collisional pumping in the case of the CO_2 laser. The volumetric pump rate R_p is E_p/τ_p and is assumed constant for time τ_p . The rate of change in the upper level population due to decay and pumping is governed by:

$$\frac{dn_2}{dt} = R_p - n_2/\tau_2 \quad (\text{A17})$$

The rate of change of the lower laser level population is determined by :

$$\frac{dn_1}{dt} = f_{21} n_2/\tau_2 - n_1/\tau_1 \quad (\text{A18})$$

(A18)

Equations (A17) and (A18) are subject to the initial conditions that the two levels are unpopulated at $t = 0$ in the pumping period.

Under these conditions equations (A17) and (A18) have the solutions

$$n_2(\tau_p) = (E_p / h\nu) (\tau_2 / \tau_p) [1 - \exp(-\tau_p / \tau_2)] \quad (\text{A20})$$

$$n_1(\tau_p) = (f_{21} E_p / h\nu) (\tau_1 / \tau_p) \left[1 - \exp(-\tau_p / \tau_2) \right] \tau_2 / (\tau_2 - \tau_1) + \exp(-\tau_p / \tau_1) \tau_1 / (\tau_2 - \tau_1) \quad (\text{A21})$$

except when $\tau_1 = \tau_2$. In this case n_1 is given by

$$n_1(\tau_p) = (f_{21} E_p / h\nu) \left[\tau_1 / \tau_p - \exp(-\tau_p / \tau_p) - (\tau_1 / \tau_p) \exp(-\tau_p / \tau_1) \right] \quad (\text{A22})$$

During the optical turnaround time τ_T the decay of the two laser levels has the same form as during the pumping time, but there is now no pumping of the upper level. Equations (A17) and (A18) still describe n_1 and n_2 if R_p is set equal to zero. Now the initial conditions are determined by past changes in the laser level populations. The initial values of n_1 and n_2 are constants determined by the values of n_1 and n_2 after the previous extraction. Under these conditions equations (A17) and (A18) have the solutions:

$$\int_0^L n_{2n}(\tau_T) dz = \int_0^L n_{2n}(\tau_T=0) dz \exp(-\tau_T / \tau_2) \quad (\text{A25})$$

$$\int_0^L n_{1n}(\tau_T) dz = \int_0^L n_{1n}(\tau_T=0) dz \left[\exp(-\tau_T / \tau_2) - \exp(-\tau_T / \tau_1) \right] \times \tau_1 / (\tau_2 - \tau_1) + \int_0^L n_{1n}(\tau_T=0) dz \exp(-\tau_T / \tau_1) \quad (\text{A26})$$

where $\int_0^L n_{1n} dz$ becomes

$$\int_0^L n_{1n}(\tau_T) dz = f_{21} \int_0^L n_{22n}(\tau_T=0) dz (\tau_T/\tau_1) \exp(-\tau_T (A27) / \tau_1) + \int_0^L n_{1n}(\tau_T=0) dz \exp(-\tau_T / \tau_1)$$

when $\tau_1 = \tau_2$.

Eqn. (A16) is used to calculate the values of $\int_0^L n_{2n}(\tau_T=0) dz$ and $\int_0^L n_{1n}(\tau_T=0) dz$ in terms of the known value before the previous extraction. Eqns. (A25), (A26), and (A27) are used in eqn. (A15) to calculate the gain-length integral prior to extraction. The gain-length integral value is used in eqn. (A5) to calculate the output fluence.

IV. Results of Multipass Extraction Analysis

The multipass analysis described in section III was applied to several hypothetical systems. Different combinations of parameter values were used in order to highlight their effects on the performance characteristics. Figs. 6 to 11 show the results of this analysis.

A. Multipass Extraction Characteristics

In this section the dependence of the multipass amplifier performance on the amplifier gain, the medium degeneracy, the laser level relaxation characteristics, and the number of extraction passes will be specifically examined. To illustrate consider the fig. 6, consisting of 3 sets of curves labeled "A", "B", and "C" respectively. The set of curves labeled "A" are plots of normalized output fluence for each of a total of 4 extraction passes, and the sets labeled "B" and "C" are plots of the cumulative extraction efficiency,

$$\epsilon_{ext} = (\pi_n^o - \pi_1^i) / (E_p L) \quad (A28)$$

for each of the 4 passes. All the curves in fig. 7 are plots of cumulative extraction efficiency. All of these curves in figs. 6 and 7 are plotted against input fluence normalized to the saturation fluence. The parameters for pump time, optical turnaround time, f_{21} , and degeneracy ratio were made equal to zero in the figure 6 calculations in order to isolate the effects of optical loss.

The curves for the first extraction pass in figure 6 correspond to the $\int_0^L \omega_0 dz = 4$ curves for the single pass amplifier in figures 2 and 3. Figure 6A illustrates the increase in extracted energy possible by utilizing more than one extraction pass. This advantage is most dramatic for the lower input fluences. At inputs higher than a saturation fluence the output curves for different numbers of passes become almost indistinguishable on this scale. This is because an input fluence greater than a saturation fluence will extract a significant portion of the stored energy on the first

pass. In addition, the input fluence itself is a major part of the resulting output fluence. Differences in performance characteristics for different numbers of passes are more apparent from the extraction efficiency curves in figure 6 B. Figure 6B shows that there are clearly defined ranges where a specific number of extraction passes is optimum in terms of efficiency and output fluence. These results show that for input fluences less than a saturation fluence two or more extraction passes are favored over a single pass. However, operating a multipass system with more extraction passes than the optimum number can be heavily penalized in efficiency due to the increased optical losses to the high fluence beam between passes. This can be seen by comparing the efficiencies for different numbers of extraction passes in figs. 6B or 6C. The penalty for operating with too many extraction passes is especially true for $\Pi^i/\Pi_s > 1$, where for these conditions the single pass amplifier is highly favored. Too few passes will not extract the stored energy efficiently. Too many passes will incur heavy optical losses. Of course any specific system will be designed considering a tradeoff between the greater efficiency of operating with the optimum number of passes against the added costs of the optical and system elements to provide each additional extraction pass. For this purpose a separate calculation must be made for the specific system being considered.

As seen by comparing fig. 6B with fig. 6C, increasing the optical losses between passes by 10 percent decreases the extraction efficiency for the multipass system by roughly 10 percent. This is understandable because the higher optical loss puts greater penalties on each additional pass. For the same reason, the penalty for operating with too many passes increases substantially.

The purpose of the efficiency curves in figure 7 is to demonstrate the effects of the degeneracy ratio and gain recovery on the multipass system efficiency. To isolate these effects, the pump time and f_{21} are set equal to zero. The efficiency curves in figure 7A illustrate the dramatic effect of the degeneracy ratio in reducing efficiency for bottlenecked extraction. When $\tau_1/\tau_2 < 1$ the lower level will relax faster than the upper level. In this case the gain will actually increase or "recover" during the turnaround time. The efficiency curves in figure 7B are for an example of such gain recovery, where some of the efficiency which would be lost due to the moderate value of degeneracy ratio is regained during an appropriate optical turnaround time. Fig. 7B shows that a multipass system with gain recovery is favored over a single pass system for inputs up to nearly 10 saturation fluences. This is considerably higher than for the systems without gain recovery. It certainly includes the entire input range of practical interest. This recovery does not continue indefinitely. Eventually the lower level will be effectively relaxed and additional time will only deplete the upper level and thus the gain. Where gain recovery is possible there is an optimum value of the turnaround time which will maximize the gain. It can be calculated from eqns. (A15), (A25), and (A26) by setting the time derivative of the gain equal to

zero. Because of its appearance in equation (A3), the expression for gain, equation (A3), increasing the degeneracy ratio exaggerates any effects which depend on the behavior of the lower laser level population, including gain recovery during the turnaround time or gain degradation during the turnaround time or the pump time.

The efficiency curves in figure 7 are for an $(\alpha_0 L)_M$ value of 1.5 while those in figure 6 are for a value of 4. A comparison then of the curves in figure 6B with the top curves in figure 7A illustrates the effects of $(\alpha_0 L)_M$ variation. The higher value of $(\alpha_0 L)_M$, due to a greater pump energy deposition, will result in higher values of gain throughout the multipass extraction operation. The higher gain will result in smaller input fluences being amplified into the saturated extraction regime. As shown by comparing figs. 6B and 7A the efficiency curve for any extraction pass will then be broader for the higher value of $(\alpha_0 L)_M$. A comparison of figs. 6B and 7A also shows that the value of input fluence for which single pass extraction becomes more efficient than multipass extraction is affected only slightly by the change in $(\alpha_0 L)_M$.

During the pump time the upper level population increases from zero until the loss rate, n_2/τ_2 , equals the pumping rate R_p . The lower level population also approaches a steady value when the

loss rate, n_1/τ_1 , equals the rate of increase from upper level decay, $f_{21}n_2/\tau_2$. Depending on the specific values of g_2/g_1 , τ_1/τ_2 , and f_{21} the gain may rise monotonically to a steady value or it may have a maximum. Using a pumping time which produces as high a gain as possible will produce the highest output fluence from the subsequent extraction. However, the upper level is decaying during the entire pumping time. Therefore a tradeoff must be made between efficiency and output fluence in selecting a pumping time. The pumping rate will depend on the capacity of the pump technology and any limits to the pumping power for damage considerations. The total energy density deposited is then this limiting pump rate times the optimized pump time. For some systems it may be necessary to limit the total deposited energy density to a smaller value determined by other damage criteria. In this case the shortest possible pump time to deposit this energy density will produce the greatest efficiency and the greatest output fluence. In general the shorter the lifetime of the lower state compared with the lifetime of the upper state, the less lower state population will accumulate to degrade the gain. Where the degeneracy ratio is zero, the lifetime ratio will not matter. But for nonzero g_2/g_1 , smaller values of the lifetime ratio will lead to better amplifier performance.

B. Optimum Extraction Efficiency Profiles

As discussed in the previous section there are a large number of parameters which affect the multipass amplifier system performance characteristics. These parameters interact in a complex manner, and each may cause significant effects on the performance

characteristics in different ranges of parameter values. For this reason, one can't identify ^{only} any one or two parameters which dominate the system performance. It is possible however to form some qualitative and semi-quantitative conclusions regarding the tradeoff of the parameters. The form of the extraction equation and the expressions governing the level populations lend themselves to a reduction of the parameter space into a minimum set of key ratios and nondimensional quantities: Γ/Γ_s , τ_1/τ_2 , τ_p/τ_2 , τ_1/τ_2 , g_2/g_1 , $(\alpha_0 L)_M$, f_{21} , and T . In figures which follow, τ_1/τ_2 vs g_2/g_1 and $(\alpha_0 L)_M$ vs g_2/g_1 were chosen as pairs of key parameters to form 2 dimensional parameter spaces in which to plot efficiency profiles. A set of optimistic but reasonable values for the remaining parameters were chosen, with some variation within a figure and between figures to illustrate important parameter effects. The parameter Γ_1^i/Γ_s was limited to values of 10^{-2} since multipass configurations are most useful at lower initial input fluences. The maximum number of extraction passes which can be made is a system limitation that will be different in each case. ~~It was generally assumed to be 6 for this paper.~~ The highest efficiencies for up to 6 passes were plotted in these profiles.

In considering a multipass amplifier the designer is frequently faced with selecting a candidate laser medium. At this point in the system design process attention is focused on the medium characteristics, g_2/g_1 , τ_1/τ_2 , and f_{21} , rather than system parameters. Figures 8 and 9 are plots of efficiency profiles in $\tau_1/\tau_2 - g_2/g_1$ space to facilitate medium selection considerations. These figures show that efficiency requirements divide the $\tau_1/\tau_2 - g_2/g_1$ plane into fairly restrictive regions. As an example consider the system depicted by the solid curves in fig. 8. To achieve an extraction efficiency greater than 0.5 either the lifetime ratio must be less than 0.15 or the degeneracy ratio must be less than 0.6. For less optimistic system parameter values or for nonzero f_{21} , as illustrated in the other profiles in figs. 8 and 9, this bounding value of τ_1/τ_2 or g_2/g_1 is even more tightly ^{CON}unstrained. As depicted in fig. 8 8 became fairly insensitive to the degeneracy ratio for extraction efficiencies greater than 0.5 values greater than 0.6 and highly insensitive to the lifetime ratio for values above 0.15. For larger lifetime ratios the lower level lifetime has become greater than the time during ^which there is a significant upper level population. Then there is insignificant decay of the lower level. Further increases in lower level lifetime can have no effect on the gain and therefore none on the efficiency. Conversely the insensitivity to the degeneracy ratio is physically due to gain recovery counteracting the degeneracy ratio's constraint on extraction. A small decrease in lifetime ratio will have a large influence on the gain recovery. It will thus counterbalance large increases in the degeneracy ratio, and the extraction efficiency

will lack sensitivity to g_2/g_1 .

In optimizing a system design the various systems parameters must be traded off against each other. Figures 10 and 11 were included to facilitate this process. In figures 10 and 11 efficiency profiles are plotted in $(\alpha_0 L)_M - g_2/g_1$ space to examine how the amount of pumping trades off against other system parameters. For a multipass system limited to 6 extraction passes and with reasonable optical loss between passes $(\alpha_0 L)_M$ must be above 1 for the efficiency to be above 0.5. For $(\alpha_0 L)_M$ between 1 and 2 the extraction efficiency is relatively insensitive to variation in g_2/g_1 compared with variation in $(\alpha_0 L)_M$. For $(\alpha_0 L)_M$ above 2 the extraction efficiency becomes more sensitive to variation in g_2/g_1 than the variation in $(\alpha_0 L)_M$. The same general conclusions are reached if τ_p/τ_2 is paired with $(\alpha_0 L)_M$ to produce a set of profiles.

For example consider the situation when the degeneracy ratio is zero. Then the lower level population has no effect on the extraction characteristics. The energy stored in the upper laser level will be depleted by the laser beam extraction and by the upper level decay during each turnaround time period. And with each additional extraction pass optical loss depletes the energy from the laser beam. A higher value of $(\alpha_0 L)_M$ will result in a higher

The characteristic shape of these curves is due to the rapidly diminishing effect of $(\alpha_0 L)_M$ on the extraction efficiency. ~~When~~

amplification of the laser beam, as discussed in Section. II. This will reduce the number of passes required to amplify the beam into the saturated extraction regime of efficient extraction. Fewer extraction passes result in smaller optical losses and upper level decay. Thus a given portion of the stored energy can be extracted with higher efficiency for a higher $(\alpha_0 L)_m$. The number of extraction passes required to achieve a given amplification is approximately inversely proportional to the gain-length. So the increase in efficiency with increased $(\alpha_0 L)_m$ diminishes quickly as $(\alpha_0 L)_m$ becomes large. This is especially true when the total number of extraction passes becomes very small.

If the degeneracy ratio increases, the $1/(1 + g_2/g_1)$ factor in the extraction efficiency causes a strong decrease in efficiency. To maintain the same efficiency along a constant efficiency profile $(\alpha_0 L)_m$ must increase at a nonlinear rate with the degeneracy, as shown in figures 10 and 11. As $(\alpha_0 L)_m$ becomes large it must increase at an extreme rate to maintain a given value of efficiency.

If the optical loss and losses due to upper level decay are negligible, the efficiency profiles in figures 10 and 11 would approach limits of constant values of g_2/g_1 . These limits can be calculated from $(g_2/g_1)_{\text{limit}} = (1 - \epsilon)/\epsilon$, where ϵ is the efficiency of a given profile. For example these limits are $g_2/g_1 = 1$ for the 0.5 efficiency profile and 0.429 for the 0.7 profile. When the optical and decay losses are nonzero, these constant degeneracy limits will decrease. On the other hand gain recovery can cause the limits to increase. For the conditions represented by the solid lines in figure 10 the 0.5 profile reaches

a limit of greater than 1 due to gain recovery. But since gain recovery diminishes for smaller degeneracy ratio, the 0.7 profile limit is less than 0.429, *because losses have decreased it.*

V. Performance Characteristics of Specific Multipass Amplifier

Systems

In order to evaluate any specific multipass system a specific calculation of output fluence and extraction efficiency, as discussed in Section III, must be performed. Figures 12 through 15 are examples of such calculations made for specific systems which have been considered as laser fusion candidates.

In analyzing real systems the extraction may not be uniform across the amplifier cross section as assumed in the analysis in sections II and III. This nonuniformity is typically due to the extracting laser beam having a nonuniform cross sectional profile or to the energy deposition being nonuniform during the pumping process. These nonuniformities can be handled by dividing the amplifier cross section into small elements, each of which has an approximately uniform cross sectional profile. The final output fluences are then averaged over all the cross sectional elements.

✓ Pumping (any) nonuniformity along the amplifier axis will be integrated out in the gain-length integral. The example calculations in figures 12-15 have taken these nonuniformities into account when appropriate.

Figures 12 and 13 plot extraction efficiency and output fluence against input fluence for a V:MgF₂ medium with a nonuniform extracting pulse profile.³ At a moderate level of pumping, $(\alpha_0 L)_m = 2$, the V:MgF₂ system can deliver output fluences exceeding nominal damage limits with 0.7 extraction efficiency for reasonable input fluences and with 4 or fewer extraction passes. The Tm:Glass system in figure 14,³ on the other hand is limited to less than 0.5 extraction efficiency for similar input fluences and the Selenium (Group VI) system in figure 15^{2,4} produces only slightly greater than 0.5 efficiency even though it has a larger gain-length product, $(\alpha_0 L)_m = 3$. The disparity in these system performances can be attributed primarily to differences in their medium characteristics. The V:MgF₂ system is phonon terminated, which means that the lower level lifetime is essentially zero and the degeneracy ratio is zero to account for the completely unbottlenecked extraction. The Tm:Glass system has a degeneracy ratio of approximately 0.55 and a laser level lifetime ratio τ_1/τ_2 of 25. For the Selenium system the degeneracy ratio is 0.75 and the lifetime ratio is approximately 0.2. Locating these points in the parameter space of figure 8 and 9 shows that the V:MgF₂ system is capable of greater than 0.7 extraction efficiency (for a uniform beam profile) while the Selenium and Tm:Glass systems are near the 0.5 efficiency profile only for the more optimistic system parameters.

VI. Summary

This paper has examined laser amplifier extraction from a storage medium. Two general approaches were considered: a single

pass amplification of the laser beam and a multipass amplifier system where the laser beam is returned through the medium for additional extraction one or more times following the initial pass. The multipass technique provides the opportunity to extract energy from upper laser level states missed during the first pass. For this reason it has the significant advantage over the single pass amplifier of providing high energy gain and high extraction efficiency simultaneously for a wide range of parameter values.

→ For a wide range of practical values of amplifier parameters the multipass amplifier configuration is ^{generally} favored when the input fluence is less than a saturation fluence. Multipass amplifier systems with significant gain recovery can be superior to a ^N simple pass amplifier for all values of input fluence of practical interest. Multipass performance characteristics depend on the medium and system parameters through their influence on the input fluence to each extraction pass and on the gain-length integral. Optical losses between passes reduce efficiency and can heavily penalize systems using too many extraction passes. During the pump time or between passes decay of the energy stored in the upper laser level will decrease the gain-length integral and therefore the efficiency of extraction.

When there is no gain recovery

For bottlenecked extraction without gain recovery a nonzero degeneracy ratio will limit the extraction process and hence the extraction efficiency. When the lower laser level population decays faster than the upper level population, gain recovery can remove some of this limitation on extraction. Under these conditions there is an optimum value of optical turnaround time which will produce the maximum improvement in efficiency.

An increase in $(\alpha_0 L)_M$ due to greater pump energy deposition will improve the efficiency. This improvement diminishes rapidly with larger values of $(\alpha_0 L)_M$.

A given acceptable value of extraction efficiency places severe restrictions on the possible values of either the degeneracy ratio or the laser level lifetime ratio. On the other hand the extraction efficiency is insensitive to a large range of values of either the degeneracy ratio or the lifetime ratio.

References

W. H. Lowdermilk and J. E. Murray, "The Regenerative Amplifier: I - Theory and Numerical Analysis," to be published in J. of Appl. Phys., manuscript no. 8829R.

R. A. Haas, "Laser System Architectures - Energy Extraction," Laser Program Annual Report - 1977, Lawrence Livermore National Laboratory, Report UCRL-50021-77 (1978), p. 7-13.

W. F. Krupke, Lawrence Livermore National Laboratory, Livermore, CA, private communication.

4. R. A. Haas, "Group VI Laser System Analysis," Laser Program Annual Report - 1977, Lawrence Livermore National Laboratory, Report, UCRL-50021-77 (1978), p. 7-40.

Figure Captions

1. Laser Amplifier Energy Extraction Configurations.
2. Single Pass Amplifier Performance Characteristics. Normalized output fluence is plotted as a function of normalized input fluence for several values of the gain length integral.
3. Single Pass Amplifier Performance Characteristics. Normalized extraction efficiency is plotted as a function of normalized input fluence for several values of the gain-length integral.
4. Single Pass Amplifier Performance Characteristics. The fraction of the pump energy density extracted by the laser beam is plotted as a function of the normalized position along the amplifier axis for several values of the normalized input fluence. The position is normalized as the gain-length.
5. Three level laser model for multipass amplifier extraction analysis.

6. Performance Characteristics of a Multipass Amplifier when

$(\alpha_0 L)_m = 4, \tau_1/\tau_2 = 0.1, \text{ and } g_2/g_1 = \tau_1/\tau_2 =$

U.C. $\tau_p/\tau_2 = \tau_1/\tau_2, f_{21} = 0$. This figure is divided into three sets of curves. Set A are normalized output fluence curves for $\tau = 0.95$. Sets B and C are extraction efficiency curves for $\tau = 0.95$ and 0.85 respectively. Each curve is identified with its extraction pass number.

7. Performance Characteristics of a Multipass Amplifier when

$(\alpha_0 L)_m = 4, \tau_1/\tau_2 = 0.1, \tau_p/\tau_2 = 0, \text{ and } f_{21} = 0$.

U.C. Extraction efficiency is plotted as a function of normalized output fluence. Each curve is identified with its extraction pass number. The upper set of curves in section A of this figure *has* $\tau_1/\tau_2 = 0.1$ and $g_2/g_1 = 0$, while the lower set has $\tau_1/\tau_2 = 0$ and $g_2/g_1 = 1$. The set of curves in section B of this figure *has* $\tau_1/\tau_2 = 0.1$ and $g_2/g_1 = 1$.

has

8. Multipass Amplifier Extraction Efficiency Profiles for when

$(\alpha_0 L)_m = 4, \tau_p/\tau_2 = 0.25, \tau_1/\tau_2 = 0.05, \tau_1'/\tau_3' = 10^{-2}$. Solid

curves are for $f_{21} = 0$. Dashed curves are for $f_{21} = 1$. Each curve is identified with its efficiency. Each profile represents the maximum extraction efficiency achieved in a total of 6 passes.

MULTIPASS Amplifier

9. Extraction Efficiency Profiles for $(\alpha_0 L)_m = 2, \tau_p/\tau_2 = 0.25,$

$\tau_1/\tau_2 = 0.05, \tau_1'/\tau_3' = 10^{-2}$. Solid curves are for $f_{21} = 0$.

Dashed curves are for $f_{21} = 1$. Each curve is identified with its efficiency. Each profile represents the maximum extraction

10. Multipass Amplifier Extraction Efficiency Profiles for when

$\tau_p/\tau_2 = 0.05$, $\tau_1/\tau_2 = 0.1$, $f_{21} = 0$, $\Gamma_1^2/\Gamma_2^2 = 10^{-2}$. Solid curves are for $\tau_p/\tau_2 = 0.25$. Dashed curves are for

$\tau_p/\tau_2 = 0.50$. Each curve is identified with its efficiency.

Each profile represents the maximum extraction efficiency achieved in a total of 6 passes.

11. Multipass Amplifier Extraction Efficiency Profiles for when

$\tau_p/\tau_2 = 0.05$, $\tau_p/\tau_2 = 0.25$, $f_{21} = 1$, $\Gamma_1^2/\Gamma_2^2 = 10^{-2}$. Solid curves are for $\tau_1/\tau_2 = 0.1$. Dashed curves are for $\tau_1/\tau_2 = 0.3$.

Each curve is identified with its efficiency. Each profile

represents the maximum extraction efficiency achieved in a total of 6 passes.

12. Performance Characteristics of a V:MgF_2 Multipass Amplifier

System. Extraction efficiency is plotted as a function of input fluence when $\tau_p/\tau_2 = 0.174$, $\tau_p/\tau_2 = 0$, $\tau_1/\tau_2 = 0$, $g_2/g_1 = 0$,

$(\alpha_0)_{in} = 2.077$, $T = 0.95$ and $f_{21} = 0$. Each curve is

identified with its extraction pass number.

V.C.

15
2

13. Performance Characteristics of a V:MgF₂ Multipass Amplifier System. Output fluence is plotted as a function of input fluence. Each curve is identified with its extraction pass number.

14. Performance Characteristics of a Tm:Glass Multipass Amplifier System. Extraction efficiency is plotted as a function of input fluence when $\tau_p/\tau_2 = 0.125$, $\tau_r/\tau_2 = .025$, $\tau_1/\tau_2 = 25$, $g_2/g_1 = 0.56$, $(\alpha_0 L)_M = 1.88$, $T = 0.95$, and $f_{21} = 0$. Each curve is identified with its extraction pass numbers.

15. Performance Characteristics of a Selenium ($^{150}\text{S}_0 \rightarrow ^{3}\text{P}_1\text{0}$) Multipass Amplifier System. Extraction efficiency is plotted as a function of input fluence when $\tau_p/\tau_2 = 0.1$, $\tau_r/\tau_2 = 0.05$, $\tau_1/\tau_2 = 0.2$, $g_2/g_1 = 0.75$, $(\alpha_0 L)_M = 3.0$, $T = 0.95$, and $f_{21} = 0$. Each curve is identified with its extraction pass number.

NOTICE

This report was prepared as an account of work sponsored by the United States Government. Neither the United States nor the United States Department of Energy, nor any of their employees, nor any of their contractors, subcontractors, or their employees, makes any warranty, express or implied, or assumes any legal liability or responsibility for the accuracy, completeness or usefulness of any information, apparatus, product or process disclosed, or represents that its use would not infringe privately-owned rights.

Reference to a company or product name does not imply approval or recommendation of the product by the University of California or the U.S. Department of Energy to the exclusion of others that may be suitable.

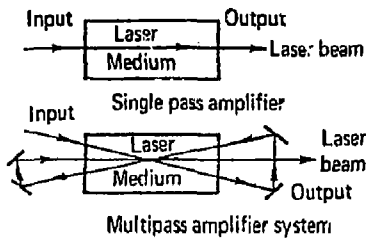


Fig. 1

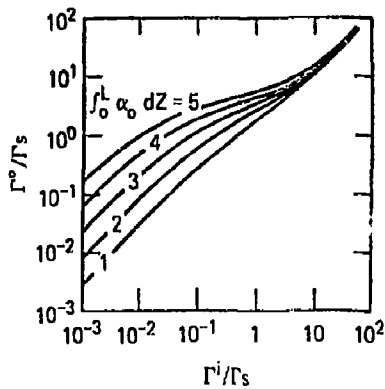


Fig. 2

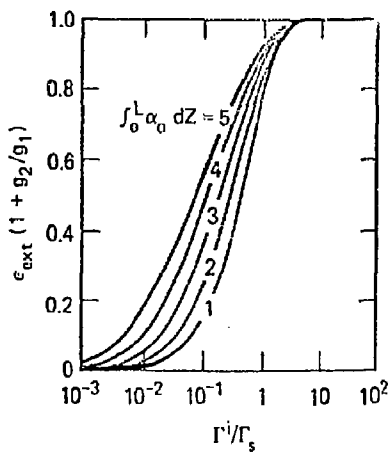


Fig. 3

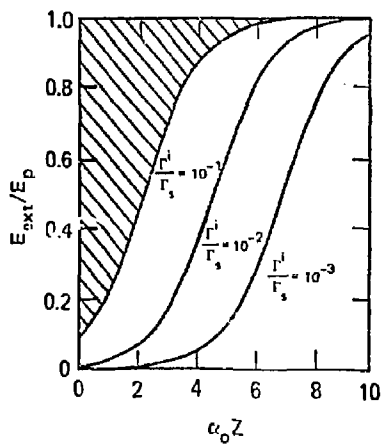


Fig. 4

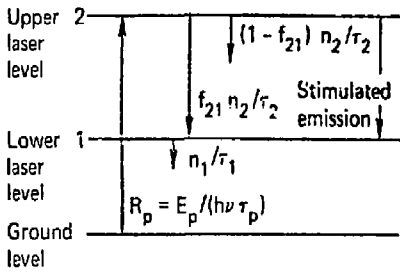


Fig. 5

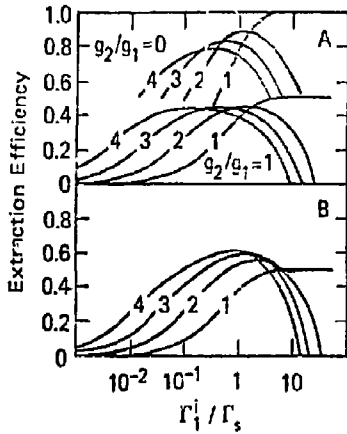


Fig. 7

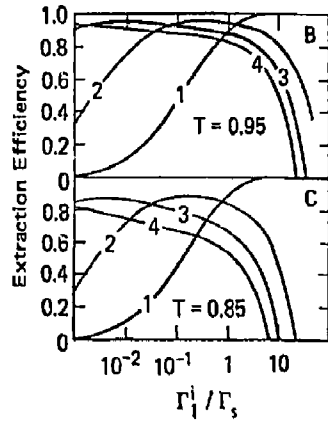
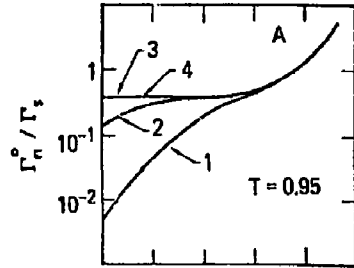


Fig. 6

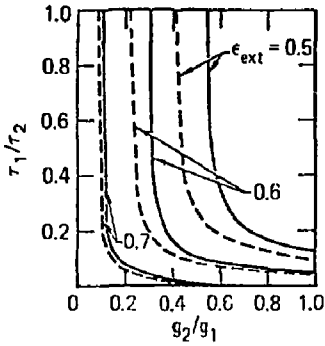


Fig. 8

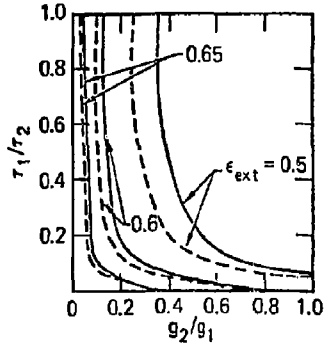


Fig. 9.

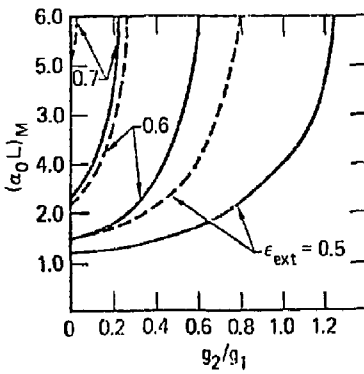


Fig. 10

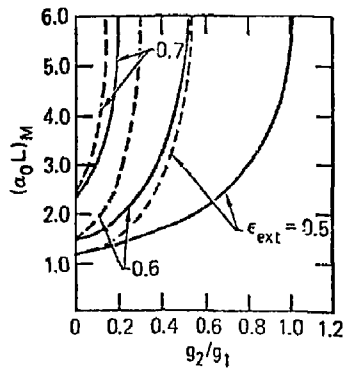


Fig. 11

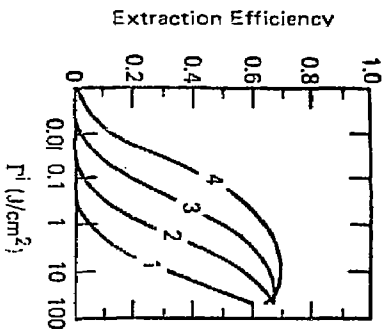


Fig. 12

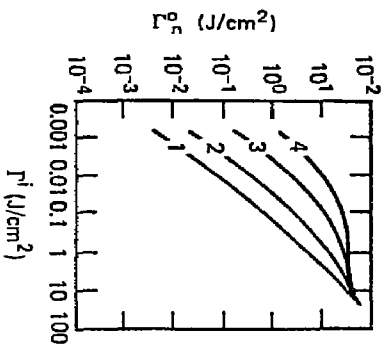


Fig. 13

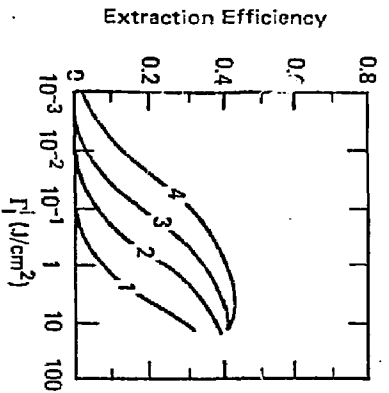


Fig. 14

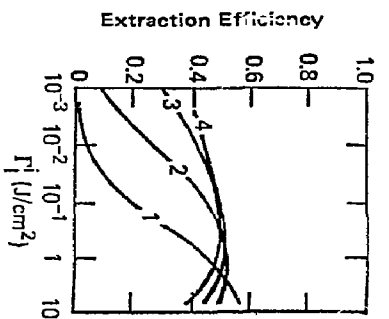


Fig. 15